

# A new route to mixed oxo/arylimido complexes of molybdenum(VI) with a tris(pyrazolyl)borate co-ligand: syntheses, spectroscopic properties and ligand-centred redox activity

Siu-Ming Lee, Ralph Kowallick, Massimo Marcaccio, Jon A. McCleverty\* and Michael D. Ward\*

School of Chemistry, University of Bristol, Cantock's Close, Bristol, UK BS8 1TS.  
 E-mail: mike.ward@bristol.ac.uk

Received 15th June 1998, Accepted 25th August 1998

Reaction of the oxo-molybdenum(V) precursor  $[\text{Mo}(\text{Tp}^{\text{Me,Me}})(\text{O})\text{Cl}_2]$  [ $\text{Tp}^{\text{Me,Me}}$  = hydrotris(3,5-dimethylpyrazol-1-yl)borate] with arylamines  $\text{RNH}_2$ , in the presence of  $\text{Et}_3\text{N}$  and air, afforded the oxo(imido)molybdenum(VI) complexes  $[\text{Mo}(\text{O})(\text{Tp}^{\text{Me,Me}})\text{Cl}(\text{=NR})]$  **1** ( $\text{R}$  = 4-tolyl), **2** ( $\text{R}$  =  $\text{C}_6\text{H}_4\text{NMe}_2$ -4); this is a new and simple route to these rare compounds. Use of 1,4-diaminobenzene afforded the mononuclear complex **3** ( $\text{R}$  =  $\text{C}_6\text{H}_4\text{NH}_2$ -4) in addition to the dinuclear complex  $[\{\text{Cl}(\text{O})(\text{Tp}^{\text{Me,Me}})\text{Mo}\}_2(\text{NC}_6\text{H}_4\text{N})]$  **4**. Reaction of various aminoferrocene derivatives  $\text{Fc-X-NH}_2$  with  $[\text{Mo}(\text{Tp}^{\text{Me,Me}})(\text{O})\text{Cl}_2]$  afforded the dinuclear ferrocenyl-molybdenum complexes  $[\text{Mo}(\text{O})(\text{Tp}^{\text{Me,Me}})\text{Cl}(\text{=NXFc})]$  **5** ( $\text{X}$  = nothing), **6** ( $\text{X}$  = 1,4- $\text{C}_6\text{H}_4$ ), **7** ( $\text{X}$  =  $\text{C}_6\text{H}_4\text{CH}=\text{CHC}_6\text{H}_4$  with all *para* substitution) and **8** ( $\text{X}$  =  $\text{C}_6\text{H}_4\text{N}=\text{NC}_6\text{H}_4$  with all *para* substitution). Reaction of  $[\text{Mo}(\text{Tp}^{\text{Me,Me}})(\text{O})\text{Cl}_2]$  with mixed amine-phenol ligands  $\text{HO-X-NH}_2$  afforded the mixed-valence complexes  $[\{\text{Cl}(\text{O})(\text{Tp}^{\text{Me,Me}})\text{Mo}\}_2(\text{=NXO})]$  **9** ( $\text{X}$  = 1,4- $\text{C}_6\text{H}_4$ ) and **10** ( $\text{X}$  = 1,5-naphthalenediyl), and the mononuclear oxo-Mo(V) complex  $[\text{Mo}(\text{O})(\text{Tp}^{\text{Me,Me}})\text{Cl}(\text{OC}_6\text{H}_4\text{NH}_2)]$  **9a** with an unreacted amino terminus was also isolated. The complexes were characterised by  $^1\text{H}$  NMR and IR spectroscopy, FAB mass spectrometry and UV/VIS spectroscopy. Whereas the simple oxo-imido-Mo(VI) cores of **1** and **5–10** undergo completely irreversible oxidations, complexes **2** and **3** undergo two reversible ligand-centred oxidations, one of the pendant amino group to give a radical cation, and the second of the imido fragment resulting in a quinonoidal structure  $\{\text{Mo}=\text{N}=\text{C}_6\text{H}_4=\text{NR}_2\}^{2+}$  ( $\text{R}$  = Me, H) for the arylimido ligand. Similarly in complex **4** the bridging fragment  $\text{Mo}=\text{NC}_6\text{H}_4\text{N}=\text{Mo}$  undergoes two reversible oxidations to give the quinonoidal dication  $\{\text{Mo}=\text{N}=\text{C}_6\text{H}_4=\text{N}=\text{Mo}\}^{2+}$  via the semiquinone radical intermediate. Spectroelectrochemical studies on **2** and **4** confirmed the nature of these reversible oxidations as ligand centred. Complexes **5** to **8** undergo a reversible oxidation of the ferrocenyl fragment, and complexes **9**, **9a** and **10** display the reversible Mo(V)/Mo(VI) and Mo(V)/Mo(IV) redox couples expected for their oxo-Mo(V) fragments.

Organoimido complexes of Mo(VI) have been of interest for a variety of reasons.<sup>1</sup> Firstly, there have been several fundamental structural and theoretical investigations regarding the nature of the molybdenum-nitrogen multiple bond, which may lie anywhere between formally double (Mo-N-C angle 120°,  $\text{sp}^2$  hybridisation at nitrogen, imido group acting as a four-electron donor with a free lone pair) and triple (Mo-N-C group linear,  $\text{sp}$  hybridisation at nitrogen, imido group acting as a six-electron donor with no lone pair) extremes.<sup>2</sup> Secondly, the electronic equivalence of oxo [ $\text{O}^{2-}$ ] and imido [ $\text{NR}^{2-}$ ] groups means that catalysis involving imido-group transfer to unsaturated organic substrates is possible in the same way as is well known for oxo-group transfer.<sup>3</sup> Thirdly, they can be effective catalysts for alkene metathesis/polymerisation reactions.<sup>4</sup>

In contrast to the large number of such imido-Mo(VI) and diimido-Mo(VI) complexes, and the even larger number of their oxo- and dioxo-Mo(VI) analogues, mixed oxo-imido-Mo(VI) complexes are surprisingly rare.<sup>3,5–10</sup> As part of our general interest in the chemistry of tris(pyrazolyl)borate complexes with molybdenum in various oxidation states, and their electrochemical,<sup>11</sup> magnetic<sup>12</sup> and optical properties,<sup>13–15</sup> in this paper we describe the preparation and properties of a series of mono- and di-nuclear oxo-imido-Mo(VI) complexes of the form  $[\text{Mo}^{\text{VI}}(\text{O})(\text{Tp}^{\text{Me,Me}})\text{Cl}(\text{NR})]$  [ $\text{Tp}^{\text{Me,Me}}$  = hydrotris(3,5-dimethylpyrazolyl)borate], from reaction of the oxo-Mo(V) precursor  $[\text{Mo}^{\text{V}}(\text{O})(\text{Tp}^{\text{Me,Me}})\text{Cl}_2]$  with primary amines  $\text{RNH}_2$ . This represents an entirely new route into oxo-imido-Mo(VI) chemistry, and apart from a single previous example<sup>8</sup> this is the first series

of such complexes which also contain a tris(pyrazolyl)borate co-ligand.

## Experimental

### General details

$[\text{Mo}(\text{O})(\text{Tp}^{\text{Me,Me}})\text{Cl}_2]$ ,<sup>16</sup> 4-ferrocenylaniline (for **6**),<sup>15</sup> 4-amino-4'-ferrocenylstilbene (for **7**)<sup>13</sup> and 4-amino-4'-ferrocenylazobenzene (for **8**)<sup>14</sup> were prepared according to published procedures. Other reagents were obtained from the usual commercial sources and used as supplied.

The following instruments were used for routine spectroscopic and electrochemical analysis:  $^1\text{H}$  NMR spectroscopy, a JEOL Lambda-300 spectrometer; electron-impact (EI) and fast-atom bombardment (FAB) mass spectrometry, a VG-Autospec instrument; UV/VIS spectrophotometry, Perkin-Elmer Lambda 2 or Lambda 19 spectrophotometers; FT-IR spectrometry, a Perkin-Elmer 1600 spectrometer. Electrochemical measurements were made using a PC-controlled EG&G-PAR 273A potentiostat. A conventional three-electrode cell was used, with Pt-wire working and counter electrodes, and an SCE reference. Ferrocene was added as a calibrant after each set of measurements, and all potentials are quoted relative to the ferrocene-ferrocenium couple.

### Spectroelectrochemical studies

The UV/VIS spectroelectrochemical studies were carried out in

**Table 1** Characterisation data for the new complexes

Complex	Colour	Yield (%)	Analysis (%)			FAB-MS M <sup>+</sup> (m/z)	IR/cm <sup>-1</sup>	
			C	H	N		$\nu_{\text{B-H}}$	$\nu_{\text{Mo-O}}$
<b>1</b>	Brown	40	46.0 (46.1)	5.4 (5.3)	17.9 (17.8)	551	2548	889
<b>2</b>	Brown	35	48.1 (47.7)	5.7 (5.7)	18.9 (19.3)	580	2547	890
<b>3</b>	Brown	38	45.1 (45.7)	5.0 (5.1)	18.2 (17.8)	552	2548	889
<b>4</b>	Dark brown	13	43.3 (43.5)	5.2 (4.8)	18.7 (18.3)	994	2542	890
<b>5</b>	Blue	10	45.9 (46.7)	4.9 (4.9)	15.7 (15.2)	645	2547	898
<b>6</b>	Purple-red	45	51.8 (51.7)	5.0 (5.0)	13.0 (13.6)	721	2546	892
<b>7</b>	Brown	10	57.0 (57.0)	5.3 (5.0)	11.4 (11.9)	823	2536	885
<b>8</b>	Brown	10	53.6 (54.0)	4.9 (4.8)	15.0 (15.3)	825	2546	894
<b>9</b>	Brown	15	43.0 (43.5)	5.1 (4.9)	17.8 (18.4)	996	2547	952, 892
<b>9a</b>	Green	35	45.4 (45.5)	5.3 (5.1)	17.0 (17.7)	554	2541	939
<b>10</b>	Dark Brown	15	46.6 (46.0)	5.0 (4.8)	15.4 (15.0)	1046	2543	946, 888

an OTTE (optically transparent thin layer electrode) cell which was built according to the design of Yellowlees *et al.* with some modifications.<sup>17</sup> The body of the cell is constructed from PTFE. The cuvette was custom-built by Heraeus Silica and Metals Ltd. (Byfleet, England) from Infrasil quartz; it has an optical path length of *ca.* 0.3 mm, and a reservoir area attached to the top to hold the reference and auxiliary electrodes. Additional Infrasil quartz windows (0.4 mm thick) on either side of the cuvette create compartments immediately adjacent to the cuvette. Temperature control was achieved by using two N<sub>2</sub> flows, one at room temperature and one which was cooled (by passing it through a coiled tube in a dewar of liquid N<sub>2</sub>), being passed through these compartments in contact with the cuvette optical surfaces. The tube carrying the cold N<sub>2</sub> was insulated to prevent ice build-up. The two flow rates could each be controlled independently by means of a needle valve (Jencons, item 313-018) attached to a flow-meter (Jencons, item 315-045) in each N<sub>2</sub> path, and by varying the relative flow rates of warm and cold components the temperature at the cuvette could be varied between room temperature and -40 °C with an accuracy of better than ±1 °C. The temperature at the cuvette was monitored with a thermocouple attached to a digital thermometer (CAL-9000). To prevent condensation on the outer surfaces of the cold Infrasil windows the sample compartment of the spectrometer was kept purged with dry N<sub>2</sub> at room temperature. The working electrode was a Pt-Rh (90:10) gauze with about 45 wires per centimetre and a wire thickness of 0.06 mm (manufactured by Engelhard-CLAL, Chessington, England); this results in an optical transparency of about 40%. The auxiliary electrode was a thick Pt wire, and the reference electrode was a Ag-AgCl electrode; these were inserted into the reservoir at the top of the cuvette, isolated from the bulk of the solvent by glass frits. The potentials were applied using an Amel model 552 potentiostat connected to an Amel model 566 function generator, and spectra were recorded approximately every 3 to 5 min until electrolysis was complete (which typically took 30–60 min). Reversibility was checked by reversing the electrolysis and ensuring that the spectrum of the starting material could be regenerated.

#### Preparations of complexes

[Mo(O)(Tp<sup>Me,Me</sup>)Cl(=NR)] (**1**, R = C<sub>6</sub>H<sub>4</sub>Me; **2**, R = C<sub>6</sub>H<sub>4</sub>NMe<sub>2</sub>; **5**, R = Fc; **6**, R = C<sub>6</sub>H<sub>4</sub>Fc; **7**, R = C<sub>6</sub>H<sub>4</sub>CH=CHC<sub>6</sub>H<sub>4</sub>Fc; **8**, R = C<sub>6</sub>H<sub>4</sub>N=NC<sub>6</sub>H<sub>4</sub>Fc; Fc = ferrocenyl). These were all prepared in an identical manner; the preparation of **1** is given here as a representative example. A solution of [Mo(O)(Tp<sup>Me,Me</sup>)Cl<sub>2</sub>] (0.200 g, 0.42 mmol), 4-methylaniline (0.090 g, 0.84 mmol) and dry Et<sub>3</sub>N (0.5 cm<sup>3</sup>) in dry toluene (20 cm<sup>3</sup>) was stirred at 70 °C for 2 d in the presence of air. The solvent was then removed *in vacuo*, and the crude purple solid was purified by column chromatography (silica, CH<sub>2</sub>Cl<sub>2</sub>); the major brown band contained the product (0.090 g, 40%).

[{Cl(O)(Tp<sup>Me,Me</sup>)Mo}<sub>2</sub>(=NC<sub>6</sub>H<sub>4</sub>O)] **9**. A mixture of [Mo(O)(Tp<sup>Me,Me</sup>)Cl<sub>2</sub>] (0.500 g, 1.04 mmol), 4-aminophenol (0.050 g, 0.46 mmol) and dry Et<sub>3</sub>N (0.8 cm<sup>3</sup>) in dry toluene (20 cm<sup>3</sup>) was heated to 80 °C for 2 d. The mixture was then cooled and the solvent removed *in vacuo* to give a brown solid, which was separated into its components by column chromatography on silica using gradient elution, starting with neat CH<sub>2</sub>Cl<sub>2</sub> and slowly increasing the polarity by addition of thf (up to 10% v/v). The first dark brown band to elute (with neat CH<sub>2</sub>Cl<sub>2</sub>) was the dinuclear complex **9** (0.077 g, 27%); with 10% thf in CH<sub>2</sub>Cl<sub>2</sub> as eluent, a green band of mononuclear [Mo(O)(Tp<sup>Me,Me</sup>)Cl(OC<sub>6</sub>H<sub>4</sub>NH<sub>2</sub>)] **9a** subsequently eluted (0.089 g, 35%).

[{Cl(O)(Tp<sup>Me,Me</sup>)Mo}<sub>2</sub>(=NC<sub>10</sub>H<sub>6</sub>O)] **10**. This was prepared in the same way as **9**, from [Mo(O)(Tp<sup>Me,Me</sup>)Cl<sub>2</sub>] (0.500 g, 1.04 mmol) and 5-amino-1-naphthol (0.073 g, 0.46 mmol). Chromatography on silica with CH<sub>2</sub>Cl<sub>2</sub> afforded **10** as a deep brown solid (0.072 g, 15%).

[Mo(O)(Tp<sup>Me,Me</sup>)Cl(=NC<sub>6</sub>H<sub>4</sub>NH<sub>2</sub>)] **3** and [{Cl(O)(Tp<sup>Me,Me</sup>)Mo}<sub>2</sub>(NC<sub>6</sub>H<sub>4</sub>N)] **4**. These were prepared in the same way as **9** and **10**, from [Mo(O)(Tp<sup>Me,Me</sup>)Cl<sub>2</sub>] (0.500 g, 1.04 mmol) and 1,4-diaminobenzene (0.050 g, 0.46 mmol). Chromatography on silica with CH<sub>2</sub>Cl<sub>2</sub> afforded dinuclear **4** as the first-eluted major product (0.070 g, 17%); further elution with 10% thf in CH<sub>2</sub>Cl<sub>2</sub> afforded mononuclear **3** (0.096 g, 38%).

Pertinent characterisation data for the complexes are collected in Tables 1 and 2.

## Results and discussion

### Synthesis and characterisation of complexes

(i) **Mono- and di-nuclear complexes containing only oxo-imido-Mo(vi) fragments.** In our earlier studies with complexes containing the {Mo(NO)(Tp<sup>Me,Me</sup>)Cl} fragment, it was found that reaction of the 16-electron [diamagnetic, formally Mo(II)] complex [Mo(NO)(Tp<sup>Me,Me</sup>)Cl<sub>2</sub>] with aromatic amines RNH<sub>2</sub> in the presence of Et<sub>3</sub>N results in displacement of one chloride ion by a deprotonated amide anion to give the products [Mo(NO)(Tp<sup>Me,Me</sup>)Cl(NHR)].<sup>18</sup> Given the parallel that has recently been drawn between the properties of nitrosyl-Mo(II) and oxo-Mo(V) complexes of tris(pyrazolyl)borates,<sup>19</sup> we were interested to see if the reaction of [Mo(O)(Tp<sup>Me,Me</sup>)Cl<sub>2</sub>] with aromatic primary amines followed a similar course.

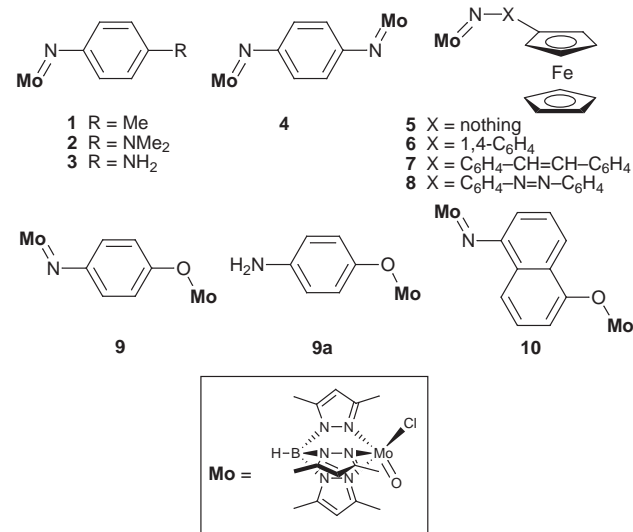
Reaction of [Mo(O)(Tp<sup>Me,Me</sup>)Cl<sub>2</sub>] with RNH<sub>2</sub> (R = C<sub>6</sub>H<sub>4</sub>Me, C<sub>6</sub>H<sub>4</sub>NMe<sub>2</sub>) in toluene in the presence of Et<sub>3</sub>N afforded in low to moderate yields diamagnetic products (**1** and **2** respectively) whose <sup>1</sup>H NMR spectra showed the presence of one aryl fragment per tris(pyrazolyl)borate [see below; the depiction of the Mo=NR linkages as bent at the N atom (rather than linear) is, in the absence of crystallographic information, arbitrary and not intended to imply anything about the order of the Mo=N bond], with no broad <sup>1</sup>H NMR signals typical of amine

**Table 2**  $^1\text{H}$  NMR data for the diamagnetic complexes (300 MHz, 293 K,  $\text{CD}_2\text{Cl}_2$ )

	Phenyl spacers	Pyrazolyl $\text{H}^5$ protons <sup>a</sup>	Pyrazolyl methyl groups <sup>b</sup>	Other protons
<b>1</b>	7.19 (4H, m)	5.91, 5.85, 5.83	2.73, 2.47, 2.42, 2.40 ( $\times 2$ ), 2.19	2.35 (3H, s; tolyl $\text{CH}_3$ )
<b>3<sup>c</sup></b>	7.31 (2H, d), 6.98 (2H, d) <sup>d</sup>	5.86, 5.79, 5.77	2.79, 2.40, 2.37, 2.36 ( $\times 2$ ), 2.25	3.14 (6H, s; $\text{NMe}_2$ )
<b>3</b>	7.34 (2H, d), 6.61 (2H, d)	5.89, 5.85, 5.83	2.71, 2.46, 2.40, 2.39 ( $\times 2$ ), 2.22	4.30 (br s, $\text{NH}_2$ )
<b>4</b>	7.06 (4H, s)	5.92 ( $\times 2$ ), 5.90, 5.89, 5.82, 5.81	2.72 ( $\times 2$ ), 2.41 ( $\times 4$ ), 2.40, 2.39, 2.26 ( $\times 2$ ), 2.24, 2.23	
<b>5</b>		5.82, 5.78, 5.70	2.76, 2.56, 2.29 ( $\times 2$ ), 2.26, 2.10	5.45, 5.23, 4.39, 4.26 (all 1H, m; $\text{C}_5\text{H}_4$ ), 4.70 (5H, s; $\text{C}_5\text{H}_5$ )
<b>6</b>	7.39 (2H, d), 7.21 (2H, d)	5.92, 5.86 ( $\times 2$ )	2.73, 2.42 ( $\times 2$ ), 2.41 ( $\times 2$ ), 2.22	4.84, 4.55 (both 2H, br s; $\text{C}_5\text{H}_4$ ) 4.15 (5H, s; $\text{C}_5\text{H}_5$ )
<b>7</b>	7.55 (2H, d), 7.47 (4H, m), 7.23 (2H, d), 7.14 (2H, m) <sup>e</sup>	5.92, 5.87, 5.84	2.74, 2.42 ( $\times 3$ ), 2.36, 2.23	4.69, 4.37 (both 2H, t; $\text{C}_5\text{H}_4$ ) 4.04 (5H, s; $\text{C}_5\text{H}_5$ )
<b>8</b>	7.92 (2H, d), 7.84 (2H, d), 7.62 (2H, d), 7.21 (2H, d)	5.94, 5.90, 5.83	2.74, 2.43 ( $\times 2$ ), 2.42, 2.30, 2.28	4.77, 4.44 (both 2H, t; $\text{C}_5\text{H}_4$ ) 4.06 (5H, s; $\text{C}_5\text{H}_5$ )

<sup>a</sup> All singlets with relative intensity 1H. <sup>b</sup> All singlets with relative intensity 3H. <sup>c</sup> Recorded in  $\text{CDCl}_3$ . <sup>d</sup> The phenyl  $\text{H}^2/\text{H}^6$  and  $\text{H}^3/\text{H}^5$  protons are not strictly 'doublets' but  $\text{A}_2\text{X}_2$  multiplets with two major components. <sup>e</sup>  $\text{CH}=\text{CH}$  protons.

protons. The FAB mass spectra were also exactly consistent with loss of both protons of the amine. The only formulation for the products consistent with these observations (and also the elemental analyses) is  $[\text{Mo}(\text{O})(\text{Tp}^{\text{Me,Me}})\text{Cl}(\text{NR})]$ , an oxo-imido-Mo(vi) complex which presumably formed by displacement of one chloride ligand of  $[\text{Mo}(\text{O})(\text{Tp}^{\text{Me,Me}})\text{Cl}_2]$  by the amide anion to give (transiently)  $[\text{Mo}(\text{O})(\text{Tp}^{\text{Me,Me}})\text{Cl}(\text{NHR})]$  [as in the nitrosylmolybdenum(II) analogues] followed by further deprotonation of the amide and aerial oxidation of the Mo(v) to Mo(vi).



The same method was used to prepare **3** and **4** by reaction of  $[\text{Mo}(\text{O})(\text{Tp}^{\text{Me,Me}})\text{Cl}_2]$  with 1,4-diaminobenzene, and these mononuclear and dinuclear complexes were again identified on the basis of their FAB mass spectra and  $^1\text{H}$  NMR spectra. For **3** the four  $\text{C}_6\text{H}_4$  protons are clearly split into two sets of two (implying the equivalence of  $\text{H}^2$  with  $\text{H}^6$ , and  $\text{H}^3$  with  $\text{H}^5$ , by free rotation of the phenyl ring with respect to the metal core) whereas for **4** they are all equivalent; also in **4** the relative integrals of the tris(pyrazolyl)borate protons are twice what they are in **3**. The low symmetry of the chiral  $\{\text{Mo}(\text{O})(\text{Tp}^{\text{Me,Me}})\text{Cl}(\text{NR})\}$  core of **1–3** means that all three pyrazolyl  $\text{H}^4$  protons, and all six methyl groups of the  $\text{Tp}^{\text{Me,Me}}$  ligand, are inequivalent in the  $^1\text{H}$  NMR spectra. In the  $^1\text{H}$  NMR spectrum of complex **4** however there are six inequivalent pyrazolyl  $\text{H}^5$  signals at *ca.*  $\delta$  5.8–5.9, and likewise there are twelve methyl group environments. This may be ascribed to the presence of two diastereoisomers arising from two (equivalent) chiral metal centres close together. However, only a single signal was observed for the central  $\text{C}_6\text{H}_4$  group.

Further support for the formulations of these complexes is

provided by two features of the IR spectra. Firstly, the Mo=O stretching vibrations occur at the rather low energy of  $890\text{ cm}^{-1}$ , which is characteristic of oxo-imido-Mo(vi) complexes<sup>3,5,8</sup> [*cf.* values of  $940\text{--}950\text{ cm}^{-1}$  for the oxo-Mo(v) fragments of **9**, **9a** and **10** below]. Secondly, the two vibrations at *ca.*  $3370$  and  $3450\text{ cm}^{-1}$  from the symmetric and asymmetric stretching modes of the  $\text{NH}_2$  groups of the free ligands have completely disappeared in the IR spectra of all of the complexes (except for **3** and **9a** which have peripheral  $\text{NH}_2$  groups). We could not definitely identify a  $\nu_{\text{Mo=N}}$  vibration: the difficulty in assigning  $\nu_{\text{Mo=N}}$  has been noted before and occurs because of (i) the variability in the Mo–N bond order, and (ii) strong coupling of the Mo=N vibration to other vibrations in the molecule, in particular the adjacent N–C vibration of the imido group.<sup>1</sup> However a value of  $1200\text{--}1300\text{ cm}^{-1}$  for  $\nu_{\text{Mo=N}}$  has been suggested,<sup>20</sup> and all of our imido-based complexes do show a strong peak in the  $1200\text{--}1250\text{ cm}^{-1}$  range which might be ascribed to  $\nu_{\text{Mo=N}}$ .

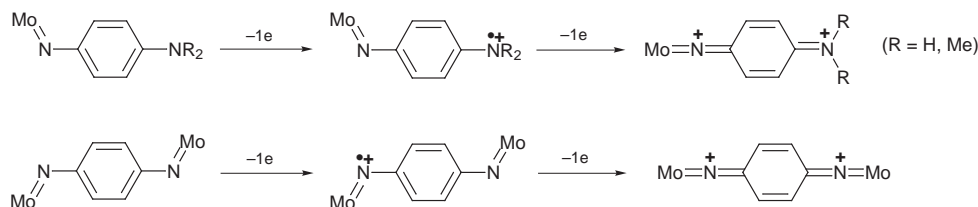
Although we were unable to obtain X-ray quality crystals of any of the new complexes, their formulation as oxo(imido)-molybdenum(vi) species from the combination of their diamagnetism and their  $^1\text{H}$  NMR, FAB-MS and IR spectra therefore seems inarguable. The formation of imido complexes by double deprotonation of amines in this way is common for many other metals but almost unknown for molybdenum,<sup>1</sup> and this route offers a simple entry into oxo-imido-Mo(vi) complexes, which previously were generally prepared from an oxo-Mo(IV) precursor by addition of an imido group from a suitable imido-transfer agent such as an organic azide.<sup>3,5</sup>

(ii) **Dinuclear complexes containing ferrocenyl or oxo-Mo(v) fragments as the second metal centre.** Using the same method we prepared the dinuclear complexes **5–8** from the appropriate aminoferrocenes. These contain an electron-donor fragment (ferrocenyl) attached to an electron-acceptor  $[\text{Mo}(\text{vi})]$  by a conjugated bridge, and are therefore related to a series of complexes we prepared recently containing ferrocenyl units linked to nitrosyl-Mo(II) fragments which showed promising non-linear optical properties.<sup>13</sup> Again all of the spectroscopic properties are consistent with the formulation of these complexes as oxo-imido-Mo(vi) species. An interesting feature of the  $^1\text{H}$  NMR spectra is that the spectrum of **5** displays four signals (relative intensity 1H each) for the substituted cyclopentadienyl ring of the ferrocenyl unit, whereas the spectra of **6–8** all display two signals of intensity 2H each. This implies that in **5** there is not free rotation about the C–N bond between the ferrocenyl group and the rest of the molecule, possibly for steric reasons because the two metal complex fragments are so close together. In **6–8** there is clearly (as expected) rotational flexibility about the phenyl spacers, such that the  $\text{C}_5\text{H}_4$  units now have twofold symmetry.

**Table 3** Electrochemical data for the complexes in CH<sub>2</sub>Cl<sub>2</sub><sup>a</sup>

	Mo <sup>VI</sup> =NR fragment			Mo <sup>V</sup> =O fragment		Ferrocenyl fragment
<b>1</b>	+1.10 (i) <sup>a</sup>		-1.63 (i)	-2.14 (i)		
<b>2</b>	+0.36 (90)	+0.73 (90)	-1.48 (i)	-1.83 (i)		
<b>3</b>	+0.39 (80)	+0.78 (80)	-1.78 (i)			
<b>4</b>	+0.86 <sup>b</sup>	+0.96 <sup>b</sup>	-1.21 (i)	-1.89 (i)		
<b>5</b>	+1.08 (i)		-1.90 (i)	-2.19 (i)		+0.20 (80)
<b>6</b>	+0.97 (i)		-1.77 (i)	-2.10 (i)		+0.05 (70)
<b>7</b>	+0.86 (i)		-1.90 (i)	-2.13 (i)		+0.10 (90)
<b>8</b>	+1.11 (i)		-1.31 (i)			+0.12 (90)
<b>9</b>	+1.21 (i)		-1.58 (i)	-2.16 (i)	-1.01 (100)	+0.57 (90)
<b>9a</b>					-1.29 (90)	+0.02 (90)
<b>10</b>	+1.10 (i)		-1.94 (i)		-1.15 (90)	+0.57 (80)

<sup>a</sup> Peak-peak separations for reversible processes (in mV) are in parentheses where appropriate; (i) denotes an irreversible process. Potentials are in vs. the ferrocene-ferrocenium couple. <sup>b</sup> Waves too close together to determine  $\Delta E_p$  values from cyclic voltammetry, but both processes are chemically reversible.

**Scheme 1**

The mixed-valence complexes **9** and **10**, prepared by reaction of [Mo(O)(Tp<sup>Me,Me</sup>)Cl<sub>2</sub>] with difunctional ligands containing phenol and amino groups, contain a paramagnetic oxo-Mo(v) fragment connected to the phenolate terminus of the bridging ligand (in accordance with the known reactivity of [Mo(O)(Tp<sup>Me,Me</sup>)Cl<sub>2</sub>] with phenolate anions)<sup>12,16</sup> and a diamagnetic oxo-Mo(vi) fragment attached to the imido terminus. During preparation of **9** we also isolated significant amounts of the mononuclear oxo-Mo(v) complex [Mo(O)(Tp<sup>Me,Me</sup>)Cl(OC<sub>6</sub>H<sub>4</sub>NH<sub>2</sub>)] **9a**. In contrast we found no evidence for formation of the other possible mononuclear complex [Mo(O)(Tp<sup>Me,Me</sup>)Cl(=NC<sub>6</sub>H<sub>4</sub>OH)], possibly because of formation of the ammonium/phenolate zwitterion as a consequence of the differing pK<sub>a</sub> values of the two groups, which would activate the phenol terminus for coordination whilst deactivating the amino terminus. NMR spectra of these complexes were not recorded because of the paramagnetism, but they gave solution X-band EPR spectra entirely characteristic of the [Mo<sup>V</sup>(O)(Tp<sup>Me,Me</sup>)Cl(OR)] group, with  $g_{\text{iso}} = 1.939$  and  $A_{\text{iso}} = 50$  G.<sup>16</sup> The IR spectra of **9** and **10** display two  $\nu_{\text{Mo-O}}$  stretching vibrations, at ca. 950 and 890 cm<sup>-1</sup>, which are characteristic of the oxo-Mo(v) and oxo-imido-Mo(vi) groups respectively as described above.

### Electrochemical properties

Very little work has been done on the electrochemical properties of complexes of this type, so we examined them by cyclic and square-wave voltammetry. The results are summarised in Table 3. The mononuclear complex **1**, the simplest representative of these oxo-imido-Mo(vi) complexes, displays completely irreversible oxidation and reduction processes. Given the +6 oxidation state of the molybdenum centre we suggest that the oxidation involves the nitrogen-based lone pair of the imido ligand, which formally carries a 2- charge. The irreversibility of the process suggests that the resulting radical cation is highly reactive and decomposes rapidly. The irreversible reductions are probably metal-centred.<sup>21</sup> These irreversible processes are broad and poorly defined in the cyclic voltammogram, and accordingly the peak potentials found by square-wave voltammetry are given in Table 3.

Complexes **2** and **3**, in which the phenylimido fragment bears NMe<sub>2</sub> and NH<sub>2</sub> substituents respectively, show two fully reversible one-electron oxidations separated by about 400 mV in each

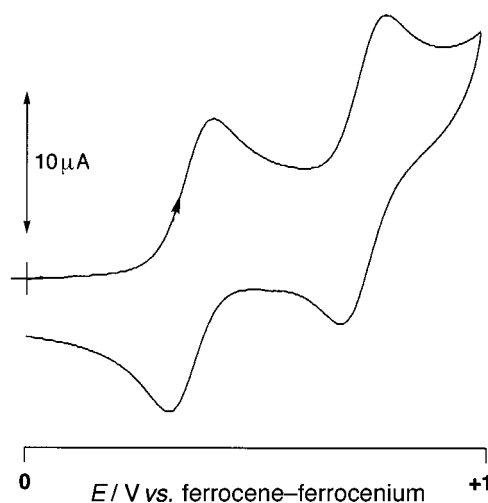


**Fig. 1** Cyclic voltammogram of **2** at a Pt working electrode in CH<sub>2</sub>Cl<sub>2</sub> (scan rate 0.2 V s<sup>-1</sup>).

case (Fig. 1). Given the additional amine substituent in each of these complexes compared to **1**, we assign these to two successive one-electron oxidations of the amino and imido ligand fragments. By comparison with the (irreversible) oxidation potential of **1** we assume that the first oxidation is based at the pendant amine site, and the second is based on the imido fragment. Formation of stable radical cations from oxidation of aromatic amines is well known,<sup>22</sup> so the reversibility of the first oxidation is understandable. Double oxidation of the 1,4-disubstituted phenyl ring will result in formation of a diamagnetic quinonoid fragment (Scheme 1). Formation of a stable structure of this sort in which the two radical sites are paired up may account for the reversibility of the second (imido-based) oxidation of **2** and **3**, which was irreversible for **1**. Irreversible reductions are also present for both complexes.

The cyclic voltammogram of complex **4** shows two overlapping oxidation waves, whose peak potentials could be resolved by square-wave voltammetry and are separated by 100 mV (Fig. 2). Although the  $\Delta E_p$  values could not individually be measured by cyclic voltammetry because of the close overlap of the two

**Table 4** Electronic spectroscopic data for the complexes in CH<sub>2</sub>Cl<sub>2</sub>

	$\lambda_{\max}/\text{nm}$ ( $10^{-3} \epsilon/\text{dm}^3 \text{mol}^{-1} \text{cm}^{-1}$ )					
<b>1</b>	242 (sh) <sup>a</sup>	291 (23)	370 (sh)* <sup>a</sup>		460 (sh)*	
<b>2</b>		284 (15)	381 (sh)	440 (26)	530 (sh)*	
<b>3</b>	248 (13)	274 (14)	359 (14)	396 (15)	500 (sh)*	
<b>4</b>	254 (18)	308 (18)	360 (sh)	430 (sh)	560 (sh)*	
<b>5</b>		286 (13)	344 (7.7)	490 (sh)	615 (2.1) <sup>b</sup>	
<b>6</b>		282 (14)	350 (14)	390 (sh)*	556 (5.0) <sup>b</sup>	
<b>7</b>	240 (sh)*		380 (34)	430 (sh)*	500 (sh)* <sup>b</sup>	
<b>8</b>	240 (sh)		396 (34)		530 (sh) <sup>b</sup>	
<b>9</b>	261 (17)	381 (13)	477 (8.7)	670 (sh)* <sup>c</sup>		
<b>9a</b>	252 (12)	388 (4.8)		655 (2.1) <sup>c</sup>		
<b>10</b>	277 (28)	418 (7.0)		600 (sh)* <sup>c</sup>		
<b>[2]<sup>+</sup></b>	289 (13)	341 (13)	429 (sh)	493 (17) <sup>d</sup>	639 (6.8) <sup>d</sup>	930 (0.8) <sup>d</sup>
<b>[4]<sup>+</sup></b>	314 (16)			556 (18) <sup>e</sup>	700 (sh)* <sup>e</sup>	950 (sh)* <sup>e</sup>
<b>[2]<sup>2+</sup></b>	268 (11)	353 (30) <sup>f</sup>	375 (sh) <sup>f</sup>			
<b>[4]<sup>2+</sup></b>	256 (14)	381 (36) <sup>f</sup>	407 (36) <sup>f</sup>	760 (sh)*		
<b>[5]<sup>+</sup></b>	255 (14)	296 (15)	462 (3.7)		890 (0.8) <sup>g</sup>	
<b>[6]<sup>+</sup></b>	254 (22)	281 (21)	410 (9.3)		896 (0.5) <sup>g</sup>	
<b>[7]<sup>+</sup></b>	256 (31)	306 (25)	384 (33)	430 (34)	930 (2.0) <sup>g</sup>	
<b>[8]<sup>+</sup></b>	245 (29)		402 (34)		802 (0.6) <sup>g</sup>	

<sup>a</sup> sh = shoulder. Those shoulders marked with an asterisk are especially poorly defined and their  $\lambda_{\max}$  values are approximate. <sup>b</sup> Ferrocenyl-based MLCT transition. <sup>c</sup> Phenolate  $\rightarrow$  Mo(v) LMCT transition. <sup>d</sup> Amine radical cation transition. <sup>e</sup> Semiquinone–diimine radical cation transition. <sup>f</sup> Quinone–diimine  $\pi \rightarrow \pi^*$  transition. <sup>g</sup> Ferrocenium-based LMCT transition.

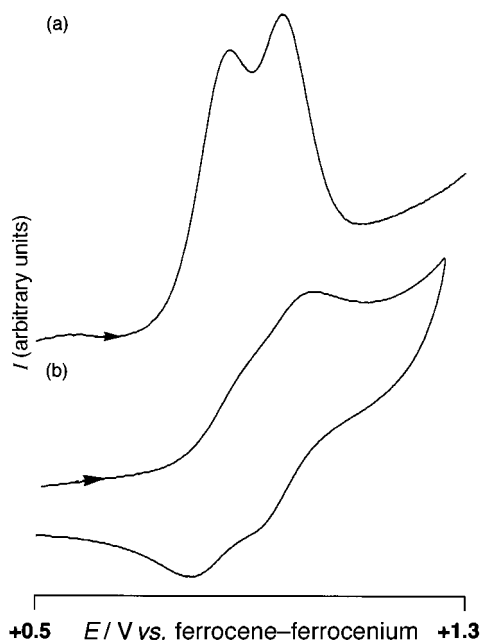


**Fig. 2** Cyclic and square-wave voltammograms of **4** at a Pt working electrode in CH<sub>2</sub>Cl<sub>2</sub> (scan rate 0.2 V s<sup>-1</sup>).

waves, the symmetry of the voltammogram (equal cathodic and anodic peak currents) suggests that both processes are chemically reversible and this was confirmed by spectroelectrochemistry (see later). The potentials of these processes are comparable to the imido-centred oxidations of **1–3**, and are clearly considerably more positive than the amino-based oxidations of **2** and **3**. We therefore ascribe these oxidations to successive one-electron oxidations of the imido fragments at either end of the bridging ligand to generate again a quinonoidal fragment (Scheme 1), which will allow the radical centres to pair up and therefore render the oxidations chemically reversible. The separation of only 100 mV between the two processes is rather small compared to other examples of electrochemical interactions across such short conjugated bridges.<sup>11,12,23</sup> This is consistent with these oxidations being based in atomic orbitals that are localised on the nitrogen atoms (formally they involve removal of one electron of the lone pair), whereas stronger electrochemical interactions and larger separations between

redox processes involve orbitals that are substantially delocalised across the bridging ligand.

The remaining dinuclear complexes display electrochemical properties which are more or less the sum of the component parts. All show the irreversible oxidation and reduction processes based on the imido-Mo(vi) fragment. In addition **5–8** show a chemically reversible ferrocenium–ferrocene couple, and **9** and **10** show the two chemically reversible metal-based couples [Mo(vi)/Mo(v) and Mo(v)/Mo(iv)] characteristic of the oxo-Mo(v)-phenolate group.<sup>12,16</sup> In complex **9a** the free NH<sub>2</sub> substituent on the aryl ring has a strongly electron-donating effect which renders the Mo(vi)/Mo(v) oxidation particularly easy; when this amino group is converted to an imido group in **9** this substituent effect is lost and the Mo(vi)/Mo(v) couple of the oxo-Mo(v) fragment is shifted positively by 0.55 V. A similar but smaller effect may be seen for the Mo(v)/Mo(iv) couple of **9a** and **9**.

### Electronic spectroscopy

The electronic spectra of the complexes are summarised in Table 4. Complex **1**, the simplest member of the set, shows an intense transition at 291 nm and then a couple of weaker shoulders on the low-energy side of the transition. For this complex we would only expect  $\pi \rightarrow \pi^*$  transitions for the aromatic ligand in the UV region, and ligand-to-metal charge transfer bands. Of the LMCT transitions, the oxo  $\rightarrow$  Mo(vi) and Cl  $\rightarrow$  Mo(vi) transitions are also expected to be in the UV region;<sup>24</sup> the imido  $\rightarrow$  Mo(vi) LMCT transition should be of lower energy than the oxo  $\rightarrow$  Mo(vi) transition because of the weaker electronegativity of N compared to O. Thus, although transitions are not individually assigned, we see the expected peaks in the UV region arising from both ligand-centred  $\pi \rightarrow \pi^*$  and LMCT transitions, with the lower-energy shoulders in the visible region possibly arising from imido  $\rightarrow$  Mo(vi) LMCT and/or pyrazolyl  $\rightarrow$  Mo(vi) LMCT transitions. For **2** and **3** the most intense transitions are at lower energy than in **1**, near 400 nm in each case, and these are likely to be imido  $\rightarrow$  Mo(vi) LMCT transitions enhanced in intensity by the presence of electron-donating NMe<sub>2</sub> and NH<sub>2</sub> substituents on the arylimido ligands. Complex **4** behaves like **1** with the most intense transition being in the UV region, and a progressively less intense series of transitions present as shoulders moving into the visible region of the spectrum.

Complex **5** has a transition at 615 nm which must arise from

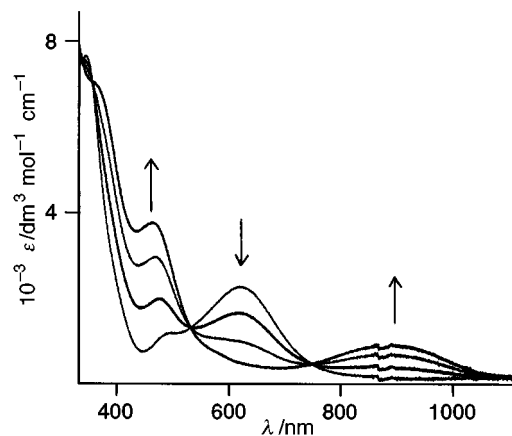


Fig. 3 Spectroelectrochemical study on the oxidation of **5** to  $[5]^+$ .

the ferrocenyl group as no such transition is present in **1–4**. Ferrocene derivatives with conjugated substituents undergo an electronic transition in the 400–500 nm region which has metal-to-ligand charge-transfer (MLCT) character, the acceptor orbital being delocalised over the cyclopentadienyl ring and the side-arm; exceptionally strongly electron-withdrawing substituents can red-shift this transition further.<sup>25</sup> We therefore assign the 615 nm transition of **5** to a ferrocenyl-based MLCT process, in which the acceptor orbital is delocalised between the cyclopentadienyl ring and the Mo(vi) substituent *via* a single-atom unsaturated bridge. In agreement with this, the transition moves to higher energy in complexes **6–8** as the Mo(vi) substituent becomes more remote from the ferrocenyl group and exerts a less pronounced electron-withdrawing effect (note also that the ferrocenyl groups of **6–8** are easier to oxidise than that of **5**, Table 3). The UV region of these spectra is more difficult to assign than those of **1–4** because of the presence of a higher-energy ferrocenyl-based MLCT transition<sup>25</sup> in addition to the ligand-centred and LMCT transitions of the Mo(vi) centre.

Complex **9a**, containing a mononuclear oxo-Mo(v) chromophore, displays the characteristic phenolate  $\rightarrow$  Mo(v) LMCT, Cl  $\rightarrow$  Mo(v) LMCT and ligand-centred  $\pi \rightarrow \pi^*$  transitions at 655, 388 and 252 nm respectively.<sup>12</sup> Complexes **9** and **10**, which contain the same chromophore in addition to an oxoimido-Mo(vi) centre, show the phenolate  $\rightarrow$  Mo(v) LMCT transition as a low-energy shoulder; the UV region will again contain a superposition of transitions characteristic of both chromophores and no attempt has been made to assign these.

### Spectroelectrochemical studies

Spectroelectrochemical studies were performed on the ferrocenyl-molybdenum complexes **5–8**, as well as complexes **2** and **4** which both showed two chemically reversible oxidations (Table 3). All measurements were made at  $-30^\circ\text{C}$  in  $\text{CH}_2\text{Cl}_2\text{-Bu}_4\text{NPF}_6$ , and all redox interconversions examined were shown to be fully chemically reversible.

Complexes **5** to **8** each undergo just one reversible redox process, the Fe(II)/Fe(III) couple of the ferrocene group. Details of the spectra recorded after this oxidation are included in Table 4, and Fig. 3 shows the results of oxidising **5** to  $[5]^+$ . The most obvious change is that the ferrocenyl-based MLCT transition at 615 nm is replaced by a new weak transition at 890 nm characteristic of the ferrocenium moiety.<sup>26</sup> Some of the higher-energy transitions are red-shifted (for example there is now a transition at 462 nm) possibly because they have Mo(vi)-based LMCT character and the Mo(vi) orbitals will be lowered further in energy by oxidation of the nearby ferrocene substituent. The same general pattern is observed for **6–8**, although the perturbation of the UV transitions following oxidation of the ferrocene moiety is less marked.

Spectra recorded during oxidation of **2** to  $[2]^+$  are shown in

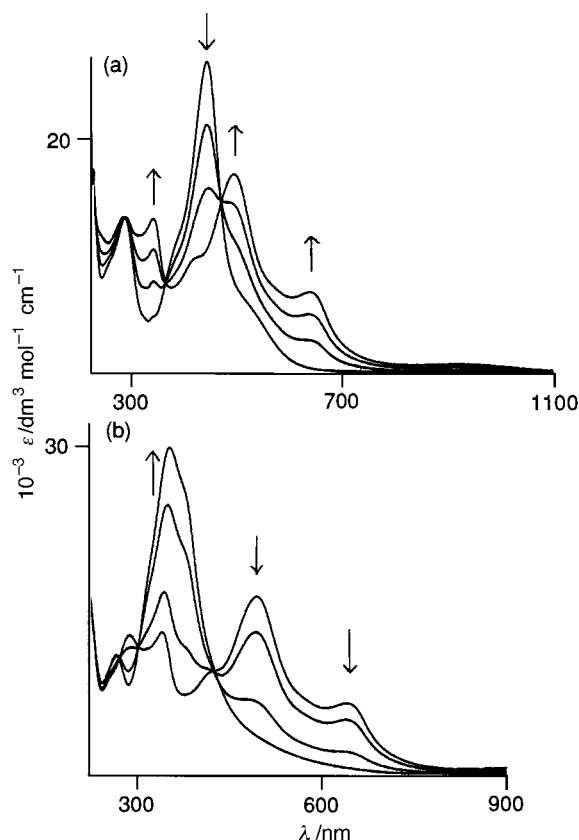


Fig. 4 Spectroelectrochemical study on (a) the oxidation of **2** to  $[2]^+$ , and (b) the oxidation of  $[2]^+$  to  $[2]^{2+}$ .

Fig. 4(a). Our earlier assignment of this first oxidation as being based on the peripheral amine substituent, generating an amine radical cation, is confirmed by the appearance of strong new transitions at 639 nm ( $\epsilon = 6800 \text{ dm}^3 \text{ mol}^{-1} \text{ cm}^{-1}$ ) and 493 nm ( $\epsilon = 17000 \text{ dm}^3 \text{ mol}^{-1} \text{ cm}^{-1}$ ). Strong absorption in the visible region is characteristic of aromatic amine radical cations, and responsible for their (usually) deep blue colour.<sup>22</sup> The radical cation of 1,4- $\text{C}_6\text{H}_4(\text{NMe}_2)_2$  for example, to which  $[2]^+$  bears an obvious similarity, has two transitions near 600 nm.<sup>27</sup> The second oxidation to give  $[2]^{2+}$  results in disappearance of these two transitions and the development of a very strong transition at 353 nm ( $\epsilon = 30000 \text{ dm}^3 \text{ mol}^{-1} \text{ cm}^{-1}$ ). This observation is consistent with oxidation of the imido nitrogen atom and consequent formation of a diamagnetic quinonoidal structure (Scheme 1); *p*-benzoquinonediimines and their derivatives have fully-allowed  $\pi \rightarrow \pi^*$  transitions in the near-UV region.<sup>28,29</sup> In fact the evolution of the electronic spectra during the two oxidations is strikingly similar to the spectral changes which occurred on oxidation of various 1,4-substituted aromatic diamines to the semiquinone-diimine radicals and then benzoquinone-diimines.<sup>28</sup>

Oxidation of **4** gave comparable results (Fig. 5). Because the two oxidation waves are so close together ( $\Delta E_p = 100 \text{ mV}$ ) we made no attempt to perform electrochemical oxidation at a potential between the two processes to give the mono-oxidised product, but performed the oxidation at a potential sufficiently positive to effect both oxidations. However, because (i) the timescale of the electrolysis is much slower than the timescale for comproportionation of fully oxidised and fully reduced species around the electrode surface, and (ii) the separation of 100 mV between the redox potentials results in a substantial comproportionation constant for the mono-cation (*ca.*  $10^4$ ), we found that we could obtain a clean spectrum of the intermediate monocation, and obtained two distinct sets of isosbestic points for the conversions  $4 \rightarrow [4]^+$  and then  $[4]^+ \rightarrow [4]^{2+}$ . The first oxidation resulted in development of a strong new

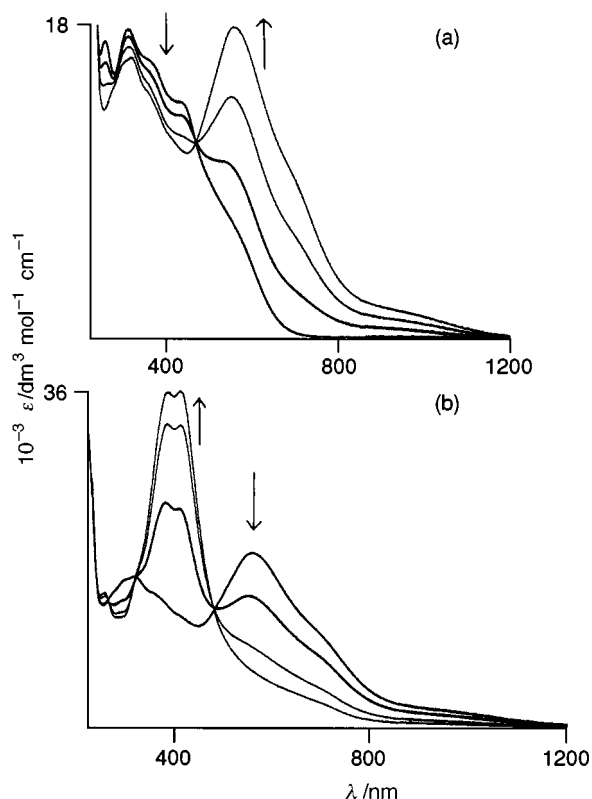


Fig. 5 Spectroelectrochemical study on (a) the oxidation of **4** to  $[4]^+$ , and (b) the oxidation of  $[4]^+$  to  $[4]^{2+}$ .

transition in the visible region, at 556 nm ( $\epsilon = 18\,000\text{ dm}^3\text{ mol}^{-1}\text{ cm}^{-1}$ ), which disappeared on the second oxidation to be replaced by a pair of more intense closely-spaced transitions in the near-UV region at 381 and 407 nm ( $\epsilon = 36\,000\text{ dm}^3\text{ mol}^{-1}\text{ cm}^{-1}$  for both). This doublet structure for the UV transition also occurs in the spectra of simple *p*-benzoquinonediimine,<sup>30</sup> and it is clear that, as for **2**, the two oxidations are ligand-centred to give a quinonoidal bridging fragment linking the two metal centres.

Although such ligand-centred redox chemistry is well known in complexes of chelating dioxolene-type ligands where interconversions between the catecholate, semiquinone and quinone oxidation levels are possible,<sup>31</sup> similar interconversions in *para*-substituted bridging ligands to give planar quinonoidal groups linking two metal ions are much less common.<sup>32</sup> A related example is provided by dinuclear oxo-Mo(v) complexes with *para*-substituted diphenolates  $[O(C_6H_4)_nO]$  as bridging ligands, where there is evidence to suggest that the two one-electron oxidations [which are formally Mo(v)/Mo(vi) couples] also have some ligand-centred character, resulting in generation of a quinonoidal bridging group.<sup>12</sup> Such complexes are of interest because the very pronounced spectroscopic changes that can occur following reversible redox interconversions may make the complexes useful as electrochromic dyes,<sup>15</sup> especially if the spectral changes occur in a region of the electronic spectrum that is accessible by diode lasers.<sup>33</sup>

## Conclusions

Reaction of  $[Mo(O)(Tp^{Me,Me})Cl_2]$  with various aromatic amines  $RNH_2$  in the presence of  $Et_3N$  and air afforded oxo-imido-Mo(vi) complexes  $[Mo(O)(Tp^{Me,Me})Cl(=NR)]$  whose electrochemical and spectroscopic properties were examined. When  $R = \text{tolyl}$  the complex undergoes a completely irreversible oxidation of the imido group. When  $R = C_6H_4NMe_2-4$  or  $C_6H_4NH_2-4$  the complexes undergo two reversible ligand-centred oxidations, to give an amine-based radical cation after the first oxidation and then a *p*-benzoquinonediimine after the second;

these assignments were confirmed by spectroelectrochemistry. Using 1,4-diaminobenzene afforded the dinuclear complex  $[Cl(O)(Tp^{Me,Me})Mo]_2(\mu\text{-NC}_6\text{H}_4\text{N})]$  which also undergoes two reversible ligand centred oxidations separated by 100 mV, to give benzosemiquinone–diimine and then benzoquinone–diimine bridging groups. Using ferrocenyl derivatives with amine substituents ( $Fc\text{-X-NH}_2$ ), dinuclear ferrocenyl–molybdenum complexes  $[Mo(O)(Tp^{Me,Me})Cl(=NXFc)]$  were also prepared in which the ferrocenyl group may be oxidised reversibly.

## Acknowledgements

We thank the Croucher foundation (Hong Kong) and the European Community TMR Network programme (contract no. EC-CHRX-CT96-0047) for financial support, and Dr M. Malaun and Dr B. Bildstein of the University of Innsbruck for providing the aminoferrocene.

## References

- 1 D. E. Wigley, *Prog. Inorg. Chem.*, 1994, **42**, 239; W. A. Nugent and B. L. Haymore, *Coord. Chem. Rev.*, 1980, **31**, 123.
- 2 C. Y. Chou, J. C. Huffman and E. A. Maatta, *J. Chem. Soc., Chem. Commun.*, 1984, 1184; B. L. Haymore, E. A. Maatta and R. A. D. Wentworth, *J. Am. Chem. Soc.*, 1979, **101**, 2063; V. C. Gibson, E. L. Marshall, C. Redshaw, W. Clegg and M. R. J. Elsegood, *J. Chem. Soc., Dalton Trans.*, 1996, 4197.
- 3 E. W. Harlan and R. H. Holm, *J. Am. Chem. Soc.*, 1990, **112**, 186.
- 4 R. R. Schrock, *Acc. Chem. Res.*, 1990, **23**, 158; R. R. Schrock, *Pure Appl. Chem.*, 1994, **66**, 1447; C. Pariya, K. N. Jayaprakash and A. Sarkar, *Coord. Chem. Rev.*, 1998, **168**, 1.
- 5 D. D. Devare and E. A. Maatta, *Inorg. Chem.*, 1985, **24**, 2846; E. A. Maatta and R. A. D. Wentworth, *Inorg. Chem.*, 1979, **18**, 2409.
- 6 J. Takacs and R. G. Cavell, *Inorg. Chem.*, 1994, **33**, 2635.
- 7 G. R. Clark, A. J. Nielson and C. E. F. Rickard, *J. Chem. Soc., Dalton Trans.*, 1996, 4265.
- 8 W. M. Vaughan, K. A. Abboud and J. M. Boncella, *J. Organomet. Chem.*, 1995, **485**, 37.
- 9 J. Chatt, R. Choukroun, J. R. Dilworth, J. Hyde, P. Vella and J. Zubieta, *Transition Met. Chem. (Weinheim, Ger.)*, 1979, **4**, 59.
- 10 M. L. H. Green, G. Hogarth, P. C. Konidaris and P. Mountford, *J. Chem. Soc., Dalton Trans.*, 1990, 3781.
- 11 A. Wlodarczyk, G. A. Doyle, J. P. Maher, J. A. McCleverty and M. D. Ward, *Chem. Commun.*, 1997, 769; J. Hock, A. M. W. Cargill Thompson, J. A. McCleverty and M. D. Ward, *J. Chem. Soc., Dalton Trans.*, 1996, 4257; A. M. W. Cargill Thompson, D. Gatteschi, J. A. McCleverty, J. A. Navas Badiola, E. Rentschler and M. D. Ward, *Inorg. Chem.*, 1996, **35**, 2701.
- 12 V. A. Ung, A. M. W. Cargill Thompson, D. A. Bardwell, D. Gatteschi, J. C. Jeffery, J. A. McCleverty, F. Totti and M. D. Ward, *Inorg. Chem.*, 1997, **36**, 3447; V. A. Ung, D. A. Bardwell, J. C. Jeffery, J. P. Maher, J. A. McCleverty, M. D. Ward and A. Williamson, *Inorg. Chem.*, 1996, **35**, 5290.
- 13 B. J. Coe, T. A. Hamor, C. J. Jones, J. A. McCleverty, D. Bloor, G. Cross and T. L. Axon, *J. Chem. Soc., Dalton Trans.*, 1995, 673; B. J. Coe, J.-D. Foulon, T. A. Hamor, C. J. Jones, J. A. McCleverty, D. Bloor, G. H. Cross and T. L. Axon, *J. Chem. Soc., Dalton Trans.*, 1994, 3427.
- 14 B. J. Coe, C. J. Jones, J. A. McCleverty, D. Bloor and G. Cross, *J. Organomet. Chem.*, 1994, **464**, 225.
- 15 S.-M. Lee, M. Marcaccio, J. A. McCleverty and M. D. Ward, *Chem. Mater.*, in the press.
- 16 W. E. Cleland, Jr., K. M. Barhhardt, K. Yamanouchi, D. Collison, F. E. Mabbs, R. B. Ortega and J. H. Enemark, *Inorg. Chem.*, 1987, **26**, 1017.
- 17 S. A. MacGregor, E. McInnes, R. J. Sorbie and L. J. Yellowlees, in *Molecular Electrochemistry of Inorganic, Bioinorganic and Organometallic Compounds*, eds. A. J. L. Pombiero and J. A. McCleverty, *NATO ASI Series C*, Kluwer Academic Publishers, 1993, vol. 385, pp. 503–517.
- 18 S. M. Charsley, C. J. Jones, J. A. McCleverty, B. D. Neaves, S. J. Reynolds and G. Denti, *J. Chem. Soc., Dalton Trans.*, 1988, 293; S. M. Charsley, C. J. Jones and J. A. McCleverty, *Transition Met. Chem.*, 1986, **11**, 329; N. J. Al-Obaidi, S. L. W. McWhinnie, T. A. Hamor, C. J. Jones and J. A. McCleverty, *J. Chem. Soc., Dalton Trans.*, 1992, 3299.
- 19 B. L. Westcott and J. H. Enemark, *Inorg. Chem.*, 1997, **36**, 5404.

- 20 K. Dehnicke and J. Strähle, *Angew. Chem., Int. Ed. Engl.*, 1981, **20**, 413.
- 21 M. Minelli, M. R. Carson, D. W. Whisenhunt, Jr., W. Imhof and G. Huttner, *Inorg. Chem.*, 1990, **29**, 4801.
- 22 S. Granick and L. Michaelis, *J. Am. Chem. Soc.*, 1940, **62**, 2241; G. Cauquis and D. Serve, *Anal. Chem.*, 1972, **44**, 2222.
- 23 M. D. Ward, *Chem. Soc. Rev.*, 1995, **24**, 121.
- 24 W. Levason, R. Narayanaswamy, J. S. Ogden, A. J. Rest and J. W. Turff, *J. Chem. Soc., Dalton Trans.*, 1982, 2009.
- 25 M. M. Bhadbhade, A. Das, J. C. Jeffery, J. A. McCleverty, J. A. Navas Badiola and M. D. Ward, *J. Chem. Soc., Dalton Trans.*, 1995, 2769; S. Toma, A. Gáplovský and I. Pavlík, *Monatsh. Chem.*, 1985, **116**, 479; S. Toma, A. Gáplovský, M. Hudecek and Z. Langfelderová, *Monatsh. Chem.*, 1985, **116**, 357.
- 26 Y. S. Sohn, D. N. Hendrickson and H. B. Gray, *J. Am. Chem. Soc.*, 1970, **92**, 3233; M. D. Rowe and A. J. McCaffery, *J. Chem. Phys.*, 1973, **59**, 3768; M. J. Carney, J. S. Lesniak, M. D. Likar and J. R. Pladziewicz, *J. Am. Chem. Soc.*, 1984, **106**, 2565.
- 27 A. Tsuchida, W. Sakai, M. Nakano and M. Yamamoto, *J. Phys. Chem.*, 1992, **96**, 8855; H. D. Burrows, D. Greatrex and T. J. Kemp, *J. Phys. Chem.*, 1972, **76**, 20.
- 28 U. Nickel, E. Haase and W. Jaenicke, *Ber. Bunsen-Ges. Phys. Chem.*, 1977, **81**, 849.
- 29 T. Uémura and M. Abé, *Bull. Chem. Soc. Jpn.*, 1937, **12**, 59; J. F. Corbett, *J. Chem. Soc. B*, 1970, 1418; H. Shizuka, Y. Sawaguri and T. Morita, *Bull. Chem. Soc. Jpn.*, 1972, **45**, 24; H. Linschitz, M. Ottolenghi and R. Bensasson, *J. Am. Chem. Soc.*, 1967, **89**, 4592.
- 30 T. Sakata, M. Hiromoto, T. Yamagoshi and H. Tsubomura, *Bull. Chem. Soc. Jpn.*, 1997, **50**, 43.
- 31 C. G. Pierpont and C. W. Lange, *Prog. Inorg. Chem.*, 1993, **41**, 381.
- 32 L. F. Joulíé, E. Schatz, M. D. Ward, F. Wever and L. J. Yellowlees, *J. Chem. Soc., Dalton Trans.*, 1994, 799; A. M. Barthram, R. L. Cleary, J. C. Jeffery, S. M. Couchman and M. D. Ward, *Inorg. Chim. Acta*, 1998, **267**, 1; F. Hartl, T. J. Snoeck, D. J. Stufkens and A. B. P. Lever, *Inorg. Chem.*, 1995, **34**, 3887.
- 33 M. Emmelius, G. Pawlowski and H. W. Vollmann, *Angew. Chem., Int. Ed. Engl.*, 1989, **28**, 1445.

Paper 8/04496A